national accelerator laboratory

FN-223
0100

BEAM BUNCH LENGTH MATCHING AT TRANSITION USING RF PHASE JUMP

W. W. Lee and L. C. Teng

February 3, 1971

The triple switch scheme was described previously by Sørenssen (CERN MPS/Int. MU/EP 66-2, 1966 and CERN MPS/Int. MU/EP 67-2, 1967). The general idea of matching beam bunch length with space charge force by manipulating the RF phase during transition crossing is here studied quantitatively and extended. The bunch length equation is similar to the one used in FN-215 and FN-215A but slightly modified.

BUNCH LENGTH (ENVELOPE) EQUATION

The equations for small phase oscillations of individual particles are (same notation as in FN-215)

$$\begin{cases} \dfrac{d\psi}{dt} = aw, & a = a(t) = \dfrac{h^2}{mR^2\gamma}\left(\dfrac{1}{\gamma_t{}^2} - \dfrac{1}{\gamma^2}\right), \\[2ex] \dfrac{dw}{dt} = -b\psi, & b = b(t) = -\dfrac{ev}{2\pi h}\cos\phi_s + \dfrac{3}{2}\dfrac{e^2Ng}{R\gamma^2}\dfrac{1}{\theta^3}. \end{cases} \tag{1}$$

The envelope equation of Equation (1) is

$$\frac{d}{dt}\left(\frac{1}{a}\frac{d\theta}{dt}\right) + b\theta - \left(\frac{S}{\pi}\right)^2 \frac{a}{\theta^3} = 0 \tag{2}$$

Two remarks are in order.

1. As shown by F. J. Sacherer (CERN/SI/Int. DL/70-12, 18.11.1970) if θ is interpreted as the rms envelope of the

Operated by Universities Research Association Inc. Under Contract with the United States Atomic Energy Commission

distribution of particles in the bunch, Eq. (2) is valid for all distributions. Also, the rms envelope depends only on the rms linear part of the space charge force which is the term included in Eq. (1) and (2).

2. We have neglected the space charge force due to the wake field such as that arising from the resistive wall. But as shown by A. Ruggiero (FN-219) this force is negligible for the NAL booster and main ring at transition.

We assume that the guide field rises linearly in time through transition. This implies that $\Delta\gamma$ per turn is constant or $v \sin \phi_s$ = constant and gives the time dependence of γ. Eq. (2) can be scaled to the simpler looking form

$$\left(\frac{y'}{f}\right)' - \left(\cot \phi_s - \frac{K}{\gamma^2 y^3}\right) y - \frac{f}{y^3} = 0 \tag{3}$$

where

$$\left\{\begin{aligned} x &= \frac{t}{T} \qquad \text{Prime} = \frac{d}{dx} \\ T &= \left(\frac{h}{2\pi} \frac{c^2}{R^2} \frac{ev}{mc^2} \sin \phi_s\right)^{-\frac{1}{2}} \\ y &= \frac{\theta}{\theta_o} \\ \theta_o &= \left(\frac{h^2}{\pi} \frac{ST}{mR^2}\right)^{1/2} \\ K &= \frac{r_p}{R} \frac{Ng}{\frac{ev}{mc^2} \sin \phi_s} \frac{3\pi h}{\theta_o^{\,3}} \\ f &= \frac{1}{\gamma}\left(\frac{1}{\gamma_t^{\,2}} - \frac{1}{\gamma^2}\right) \end{aligned}\right. \tag{4}$$

If we define $p_y \equiv \frac{y'}{f}$ we get

$$\begin{cases} y' = f\, p_y \\ p_y' = \left(\cot\phi_s - \frac{K}{\gamma^2 y^3}\right) y + \frac{f}{y^3} \end{cases} \tag{5}$$

We repeat here the physical meanings of y and p_y

$$\begin{cases} \theta = \text{envelope of } \psi = \theta_o y \\ W = \text{envelope of } w = \frac{S}{\pi\theta_o} \left(p_y{}^2 + \frac{1}{y^2}\right)^{1/2} \end{cases} \tag{6}$$

Of course, with $\phi_s = \phi_s(x)$ we are tacitly assuming that $v = v(x)$ is always so adjusted as to keep $v \sin\phi_s$ = constant. Eq. (5) is solved numerically on the computer. In general, with both γ_t- and ϕ_s- jumps we consider $\gamma_t = \gamma_t(x)$ and $\phi_s = \phi_s(x)$.

In this report we shall consider only the effect of ϕ_s-jump. All the results discussed below are for the NAL booster which has $\eta_o(0) \simeq 3.8$ and the following parameters:

$$\begin{cases} r_p = 1.53 \times 10^{-18} \text{ m} \\ g = 4.5 \\ R = 75.47 \text{ m} \\ N = 3.5 \times 10^{12} \\ \gamma_t = 5.446 \\ \Delta\gamma \text{ per turn} = \frac{ev}{mc^2} \sin\phi_s = 0.655 \times 10^{-3} \text{ (in the neighborhood of transition)} \\ S = 0.0194 \text{ eV-sec} \\ T = 2.69 \times 10^{-6} \text{ sec} \\ \theta_o = 1.405 \text{ rad} \\ K = 0.139 \end{cases}$$

THE SCHEME OF TRIPLE SWITCH

Referring to Fig. 1 where $x = 0$ at transition we see that the space charge (SC) force is defocusing (d) before transition and focusing (f) after transition; whereas the RF force is f for $\phi_s < 90^\circ$ and d for $\phi_s > 90^\circ$ before transition, and d for $\phi_s < 90^\circ$ and f for $\phi_s > 90^\circ$ after transition. All bunch length (y) curves obtained as solutions of Eq. (5) are plotted in Fig. 5. Curves (I) and (II) are the asymptotically adiabatic bunch lengths before and after transition, respectively. Our goal is to match curve (I) onto curve (II).

1. If there is no region (C) (no triple switch) the combined RF and SC forces are too strongly focusing (curve III). This makes the bunch length shrink to a minimum value way below curve (II) and enter into a rather non-linear oscillation about curve (II). This is the commonly observed beam bunch length oscillator.

2. If there is no Region (B) (no RF phase jump) the RF defocusing force always overrides the SC focusing force and the bunch length increases monotonically after transition (curve IV).

3. It is, therefore, expected that by properly adjusting the sizes of Regions (B) and (C) (namely, the values of x_1 and x_2) one can obtain matching at x_2 (curve V). The matched values are $x_1 = 26.32$ and $x_2 = 266.9$.

Because of the rather small size of Region (B) the required precision on x_1 is rather high. This may explain the fact that the triple switch scheme had only limited success when tried on the CERN PS.

OTHER SIMPLER ϕ_s-JUMP SCHEMES

A. It is evident from Fig. 1 that by properly reducing the RF defocusing force in Region (C) (increasing ϕ_s) one can eliminate Region (B) and still obtain perfect matching. This is shown in Fig. 2. The two parameters adjusted are ϕ_{so} ($>70^o$) in Region (E) and the size of Region (E) (value of x_3). The matched values are $\phi_{so} = 79.01^o$ and $x_3 = 314.1$. The resulting bunch length is plotted as curve VI in Fig. 5.

B. Moving the timing of the first ϕ_s-jump (jump from 70^o to ϕ_{so}) affects the values of ϕ_{so} and x_3. For a delayed jump, a weaker RF defocusing force, i.e., a larger ϕ_{so}, is needed for perfect matching. On the other hand, an earlier jump before transition would require a stronger RF defocusing after transition and, therefore, a smaller ϕ_{so}. In the interest of keeping the synchronous phase away from 90^o where non-linearity is largest, it is desirable to make ϕ_{so} as small as possible. The case of a minimized ϕ_{so} is shown in Fig. 3 with $x_o = -82.0$, $\phi_{so} = 76.07^o$ and $x_3 = 295.7$. The resulting bunch length is plotted as curve VII in Fig. 5.

C. We could replace the first ϕ_s-jump by a more gentle slope which can be incorporated into the RF program. An example is shown in Fig. 4 where $\phi_s(x)$ changes linearly from 70^o to a minimized $\phi_{so} = 76.73^o$ at transition, with $x_o = -112.0$ and

$x_3 = 299.6$. The corresponding bunch length is plotted as curve VIII in Fig. 5.

D. We could also replace the second ϕ_s-jump (jump across 90^o) by a gentle slope. But as pointed out in B to minimize the distortion due to non-linearity one should minimize the time spent near 90^o. It is, therefore, desirable to jump across 90^o as fast as possible.

E. Even the ϕ_s curve in Fig. 4 is still rather stylized. In practice, this will be replaced by a more realistic ϕ_s program. As long as the general feature is retained and as long as the equivalent of the parameters x_o, ϕ_{so} and x_3 are available for adjustment matching can be attained.

GENERAL EVALUATION

Compared to the γ_t-jump schemes discussed in FN-215 and FN-215A the ϕ_s-jump scheme has two major advantages.

1. The matching point x_3 to the asymptotic adiabatic curve (II) is generally much later than that for the γ_t-jump scheme. Hence, the minimum bunch length which occurs near the matching point is generally much larger. This makes the adjustment of the ϕ_s-jump scheme less critical.

2. The ϕ_s-jump scheme needs no additional equipment. The required ϕ_s programming and jump capability is normally provided in the RF system.

Of course, any matching scheme in contrast to either schemes where the bunch length oscillation due to mismatching is damped by a feed-back system or schemes where the space charge force is compensated by reactive loading of the vacuum chamber wall (see e.g., E. D. Courant, FN-187) suffers the disadvantage of not being able to follow the bunch-to-bunch or pulse-to-pulse intensity variations.

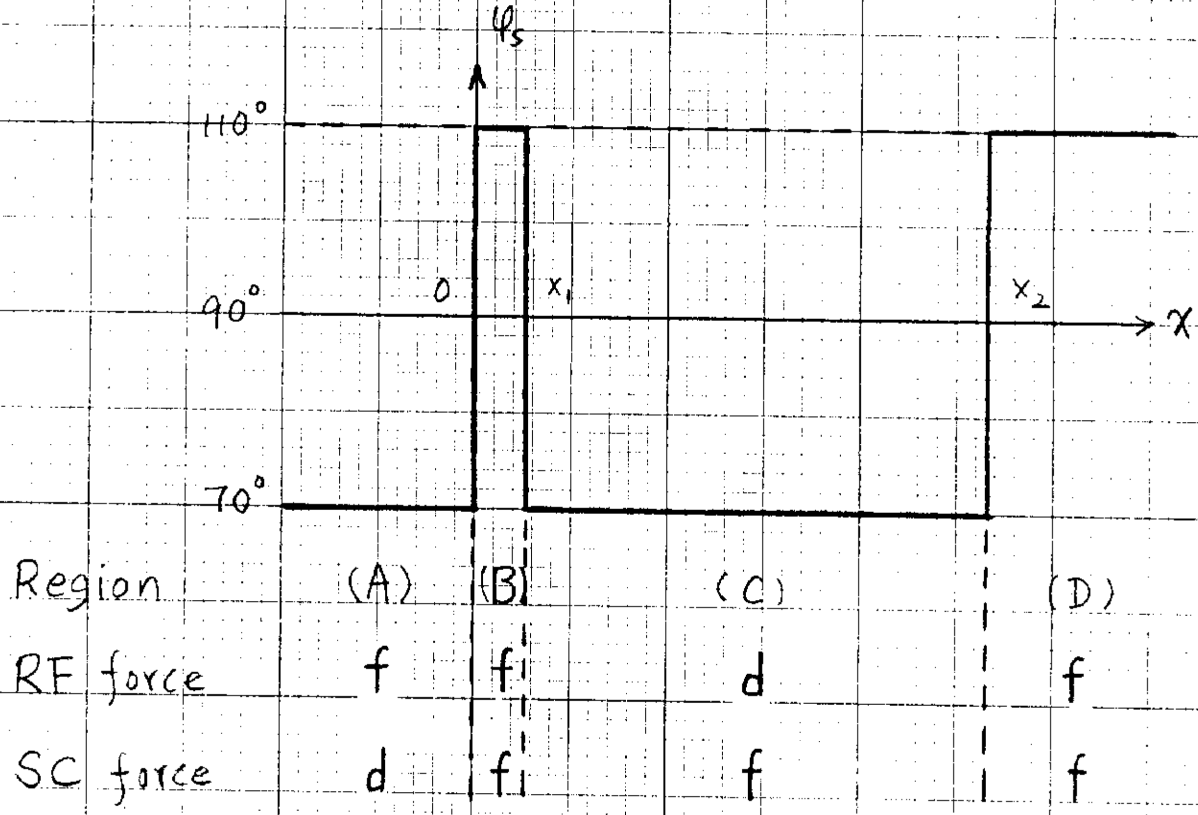

Fig. 1 Triple Switch

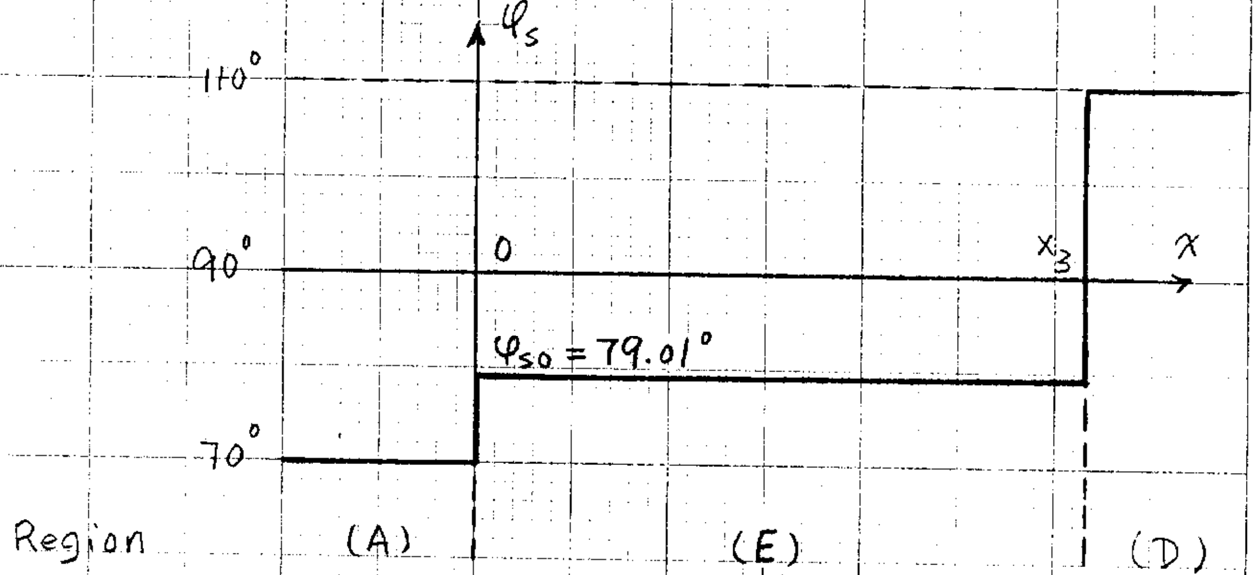

Fig. 2 Double Switch

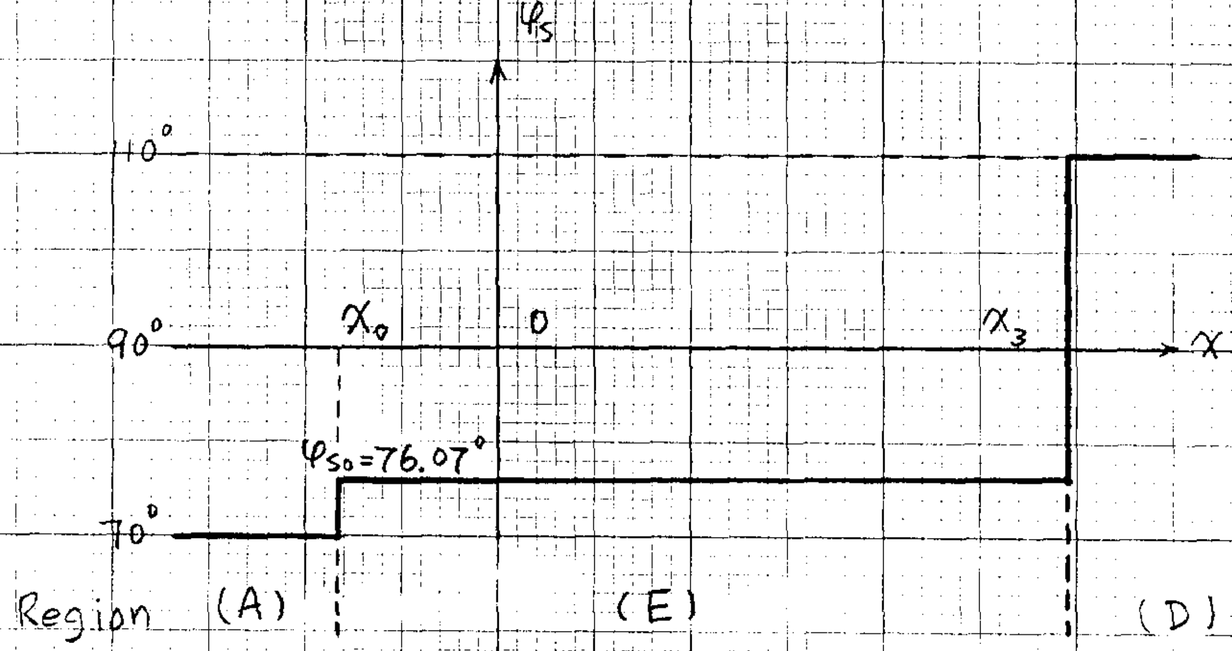

Fig. 3 Advanced Double Switch

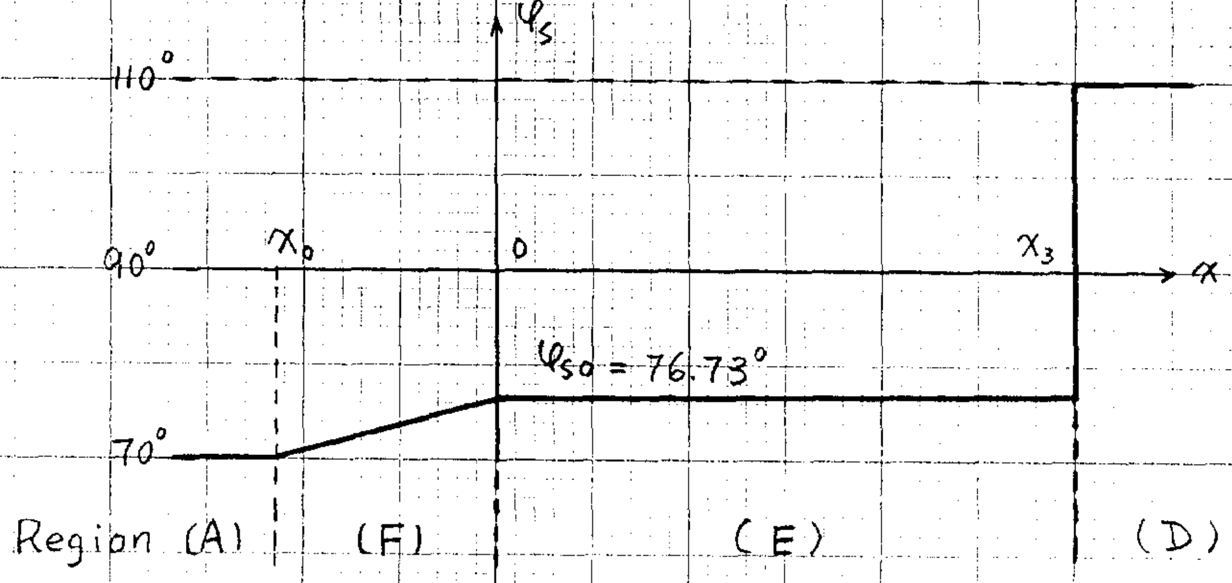

Fig. 4 A Variation of the Advanced Double Switch

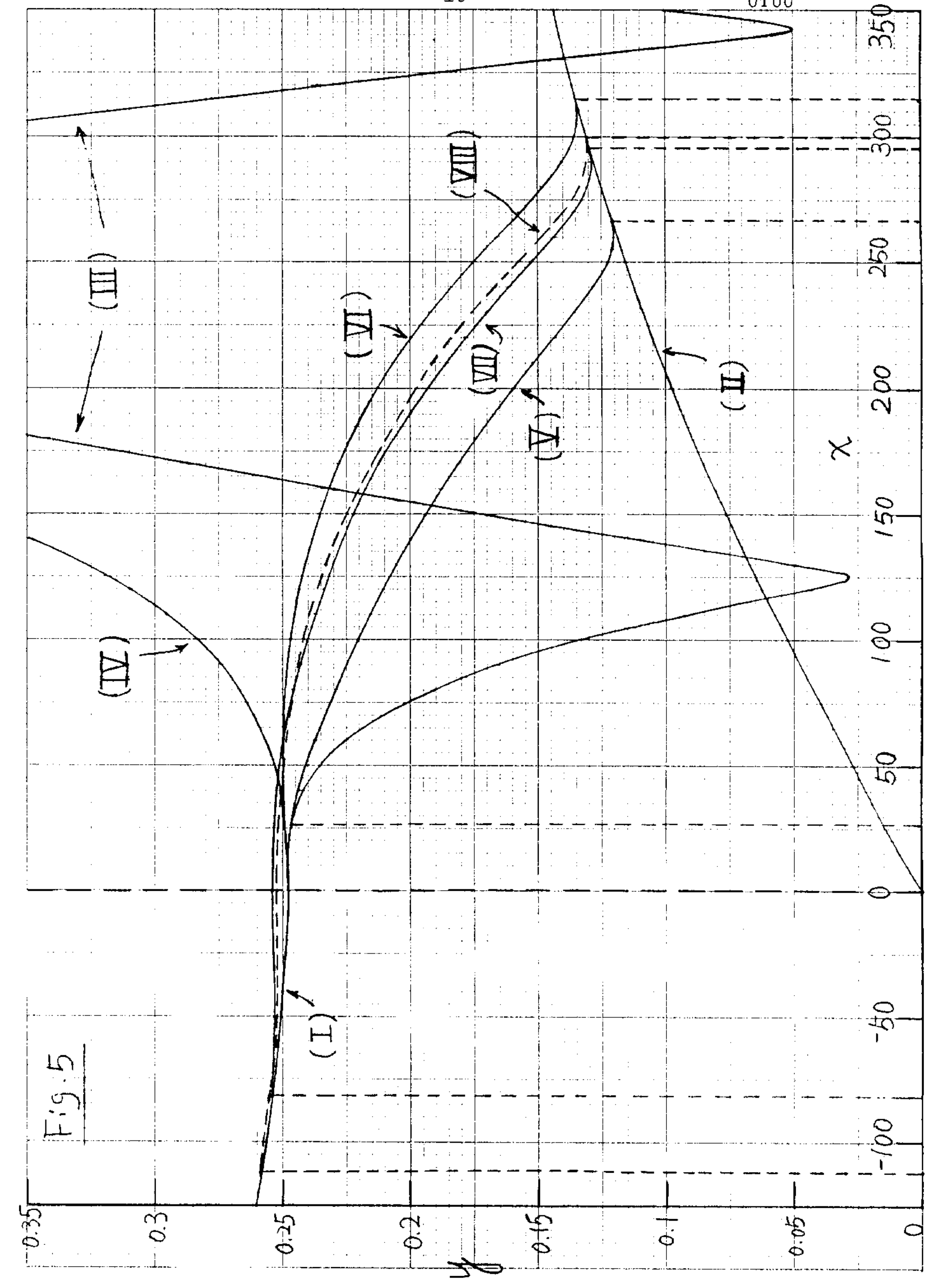
(I)
(II)
(III)
(IV)
(V)
(VI)
(VII)
(VIII)
y
x
0.35
0.3
0.25
0.2
0.15
0.1
0.05
0
-100
-50
0
50
100
150
200
250
300
350

Fig. 5

FIGURE 5

(I) Equilibrium (matched) curve before transition with $\phi_s = 70^\circ$.

(II) Equilibrium (matched) curve after transition with $\phi_s = 110^\circ$.

(III) Curve corresponding to ϕ_s given in Fig. 1 with $x_1 \to \infty$, $x_2 \to \infty$.

(IV) Curve corresponding to ϕ_s given in Fig. 1 with $x_1 = 0$, $x_2 \to \infty$.

(V) Matched curve corresponding to ϕ_s given in Fig. 1 with $x_1 = 26.32$ and $x_2 = 266.9$.

(VI) Matched curve corresponding to ϕ_s given in Fig. 2 with $\phi_{so} = 79.01^\circ$ and $x_3 = 314.1$.

(VII) Matched curve corresponding to ϕ_s given in Fig. 3 with $\phi_{so} = 76.07^\circ$, $x_o = -82.0$, $x_3 = 295.7$.

(VIII) Matched curve corresponding to ϕ_s given in Fig. 4 with $\phi_{so} = 76.73^\circ$, $x_o = -112.0$, $x_3 = 299.6$.